

**Real-time investigation of solvent swelling induced  $\beta$ -phase formation in poly(9,9-dioctylfluorene)**

M. E. Caruso

*Dipartimento di Fisica, Università del Salento, Via per Arnesano, 73100 Lecce, Italy*

M. Anni\*

*Dipartimento di Ingegneria dell'Innovazione, Università del Salento, Via per Arnesano, 73100 Lecce, Italy*

(Received 11 April 2007; revised manuscript received 6 July 2007; published 16 August 2007)

The physical processes leading to solvent swelling induced glassy- to  $\beta$ -phase transition in poly(9,9-dioctylfluorene) thin films are investigated in real time by photoluminescence and confocal spectroscopy. We show that the vapor solvent swelling induced  $\beta$ -phase formation takes place in much shorter times (few minutes) than the one usually employed in literature (several hours). Moreover, we show that the swelling is faster if the solvent mainly interacts with the PF8 aromatic rings (toluene) than with the octyl chains (iso-octane). On the contrary, no swelling is caused by nonsolvents such as *n*-butylic alcohol. Finally, we demonstrate that the  $\beta$ -phase formation is due to athermal (simultaneous) nucleation followed by diffusion controlled one dimensional crystallization.

DOI: 10.1103/PhysRevB.76.054207

PACS number(s): 42.70.Jk, 72.80.Le, 78.55.Kz, 78.66.Qn

The great interest in organic conjugated compounds is related to their potential applications in low cost electronics, optoelectronics, and photonics. Among several families of polymers showing electroluminescence,<sup>1</sup> lasing,<sup>2</sup> and field effect mobility,<sup>3</sup> polyfluorene has emerged as an attractive polymer in blue-light emitting diodes,<sup>4,5</sup> gain media in lasers<sup>6</sup> and optical amplifiers,<sup>7</sup> photovoltaic devices,<sup>8</sup> and thin film transistors.<sup>9</sup> In addition to its excellent properties for device applications, poly(9,9-dioctylfluorene) (PF8) is a very interesting system for basic photophysics studies, due to the strong morphology dependence of its optical properties. Two distinct phases are usually present in spin coated PF8 thin films, usually named as glassy and  $\beta$ -phases, with different electronic and optical properties. This feature, ascribed to a different chain geometry<sup>10</sup> of the two phases, allowed the investigation in thin PF8 films of the chain geometry dependence of the triplet<sup>11</sup> and polaron formation<sup>12</sup> and of the optical gain,<sup>13</sup> without the need for chemical modification of the molecules. Finally, as the  $\beta$ -phase photoluminescence (PL) is at lower energy than the glassy-phase one, the  $\beta$ -phase presence also modifies the relaxation processes in the film, due to the introduction of efficient glassy- $\rightarrow$  $\beta$ -phase Förster transfer (FRET), that significantly affects the emission spectra.<sup>14,15</sup> Moreover, the  $\beta$ -phase PL shows unusually narrow emission features [about 18 meV at 25 K (Ref. 16)] and an extremely well resolved vibronic structure that allowed the investigation of the origin of the PL line-width temperature dependence<sup>17</sup> and of the vibronic coupling.<sup>14</sup> Concerning the  $\beta$ -phase formation, the  $\beta$ -phase has been observed in as-deposited samples obtained by spin coating from high boiling point solvents,<sup>15,18</sup> in Langmuir-Blodgett films,<sup>19</sup> and in spin coated PF8-PMMA blends.<sup>20</sup> Moreover, the  $\beta$ -phase can be obtained in glassy-phase films by postdeposition process such as thermal treatment<sup>16</sup> or exposure to solvent vapors for several hours.<sup>14</sup> The investigation of the  $\beta$ -phase formation kinetics during postdeposition thermal cycling allowed to ascribe<sup>16</sup> the  $\beta$ -phase formation to simultaneous (athermal) nucleation, followed by one dimensional growth and crystallization, on a time scale of several hours. On the contrary, the investigation of the  $\beta$ -phase

formation process due to solvent swelling and a correlation between the  $\beta$ -phase growth and the variation of the microscopic emission properties of the PF8 thin films is still missing.

In this paper, we investigated by PL measurements the solvent swelling induced glassy- $\rightarrow$  $\beta$ -phase transition kinetics in films deposited from chloroform and then exposed to different solvent vapors, namely, toluene, iso-octane, and the nonsolvent *n*-butylic alcohol. We show that the  $\beta$ -phase formation takes place in much faster times (few minutes) than the one usually employed in literature (several hours).<sup>14</sup> In particular, we show that the solvent induced swelling is faster for toluene vapor exposure (about 4 min) than for iso-octane vapors (about 12 min). On the contrary, the  $\beta$ -phase is not formed during exposure to nonsolvents, such as *n*-butylic alcohol. We demonstrate that the swelling induced  $\beta$ -phase formation process is different from the one observed during thermal cycling.<sup>16</sup> In particular, we show that the  $\beta$ -phase is formed by athermal nucleation, followed by a diffusion controlled one dimensional (1D) crystallization. This conclusion is consistent with confocal PL maps, showing that the clusters of  $\beta$ -phase, present in the pristine sample, act simultaneously as nucleation centers for the  $\beta$ -phase formation.

PF8 (purchased from HW Sands, OHA2311) thin films were prepared by spin coating in air onto a quartz substrate from a chloroform solution 2 wt % at a spin speed of 1800 rpm for 60 s, resulting in a sample thickness of about 400 nm. Then, PL measurements were performed in real time during exposure to different solvent vapors, namely, toluene, iso-octane, and *n*-butylic alcohol. These solvents are expected to interact in different ways with the PF8 chains. In particular, toluene is expected to interact mainly with the fluorene rings, iso-octane with the octyl chains, while *n*-butylic alcohol should not interact with the PF8. For the PL measurements, we used a He-Cd ( $\lambda=325$  nm) laser exciting a circular region of the samples with a radius of about 50  $\mu\text{m}$ , with an excitation density of about 1 W  $\text{cm}^{-2}$ . The PL has been spectrally dispersed by a monochromator and

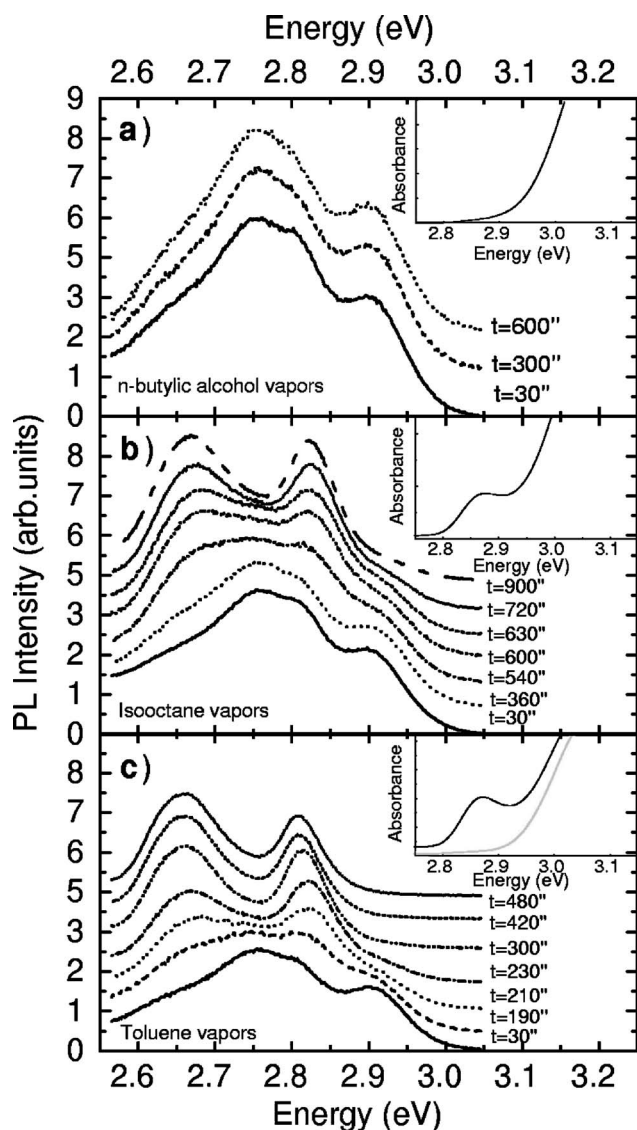


FIG. 1. PL spectra of PF8 collected at several times during exposure to toluene (bottom), iso-octane (center), and *n*-butylic alcohol (top) vapors. All the spectra are vertically translated for clarity. Inset: absorption spectra of the samples after solvent vapor exposure (black line) and of the pristine sample (gray line in the bottom inset).

detected by a Jobin-Yvon Si charge-coupled device detector as a function of time during the solvent exposure, every 30 s. The spatially resolved PL measurements were performed by an Olympus FV1000 confocal microscope. The samples were excited at room temperature in air with a solid state laser ( $\lambda=405$  nm), with an excitation density of about  $40 \text{ W cm}^{-2}$ , while the emission was collected with a photomultiplier. The absorption spectra were performed at room temperature with a UV-visible Varian spectrophotometer.

The absorption spectra of the three pristine samples, just after the deposition, show only a broad band peaked at about 3.25 eV, due to the glassy-phase  $S_0 \rightarrow S_1$  transition.<sup>21</sup> After the postdeposition treatment, a further low energy peak around 2.87 eV, which has been assigned to the  $\beta$ -phase  $S_0 \rightarrow S_1$  transition,<sup>21</sup> is observed in samples exposed to toluene

and iso-octane vapors (see inset of Fig. 1). On the contrary, this line shape change of absorption spectrum is not observed in the sample exposed to *n*-butylic alcohol.

The PL emission spectra of the three films were measured continuously during the exposure to three different solvent vapors. The PL spectrum at  $t=30$  s of the toluene exposed sample [Fig. 1(c)] shows the typical features of the glassy-phase emission with the 0-0 peak at about 2.9 eV followed by vibronic replicas at about 2.8 and 2.75 eV. Moreover, the low energy PL line shape suggests the presence of defect emission, likely related to photo-oxidation.<sup>24</sup> As the exposure time increases, we observed a fast intensity decrease of the glassy-phase PL features, together with the appearance of two new PL resonances, at about 2.82 and 2.66 eV, typical of the PF8  $\beta$ -phase PL. After about 4 min, only the  $\beta$ -phase emission is observed.

This effect is consistent with a general increase in the backbone planarity and enhancement in the effective conjugation length, due to solvent induced swelling. Similar results have been obtained for the sample exposed to iso-octane vapors, but slower  $\beta$ -phase formation is observed, as about 12 min exposure is necessary to observe only the  $\beta$ -phase PL in the spectra. On the contrary, no evidence of  $\beta$ -phase formation is obtained in the sample exposed to *n*-butylic alcohol, indicating that a nonsolvent does not induce molecule geometry variations due to swelling. We observe that the three chosen solvents have similar boiling temperatures ( $110^\circ \text{C}$  for toluene,  $99^\circ \text{C}$  for iso-octane, and  $117^\circ \text{C}$  for *n*-butylic alcohol) that ensure similar vapor densities close to the sample surface during the experiment. The observed differences in the  $\beta$ -phase formation time cannot be then trivially ascribed to different solvent molecule densities during the vapor exposure but, on the contrary, they suggest that the PF8-solvent interaction strength depends on the solvent chemical structure. In particular, this interaction is stronger with a solvent interacting with the PF8 aromatic rings (toluene) than with the one interacting with the alkyl chains (iso-octane), while negligible interactions are present with nonsolvents.<sup>22</sup>

In order to have an insight into the physical process leading to the  $\beta$ -phase formation we quantitatively investigated the glassy-  $\rightarrow$   $\beta$ -phase transition kinetics by modeling the glassy- and  $\beta$ -phase PL intensities during the phase transition. We started from the following rate equation for the glassy- and  $\beta$ -phase molecule populations:

$$\dot{n}_g = g_g - \frac{n_g}{\tau_g} - \frac{n_g}{\tau_{\text{FRET}}}, \quad (1)$$

$$\dot{n}_\beta = g_\beta - \frac{n_\beta}{\tau_\beta} + \frac{n_g}{\tau_{\text{FRET}}}, \quad (2)$$

where  $g_i$  ( $i=g$  or  $\beta$ ) describe the exciton generation due to the pump laser absorption for the glassy and  $\beta$ -phases, respectively,  $\tau_i$  is the recombination lifetime, while  $1/\tau_{\text{FRET}}$  is the glassy-  $\rightarrow$   $\beta$ -phase FRET rate. We then considered that the generation and FRET terms change during the phase transition, as the number of glassy- and  $\beta$ -phase molecules is not constant. As the generation terms are directly propor-

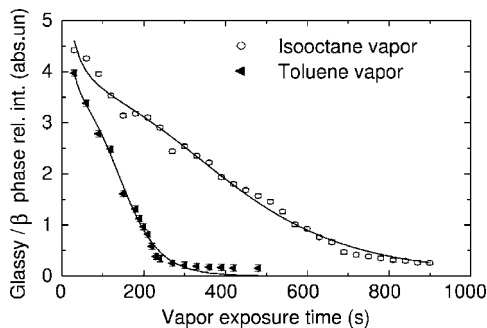


FIG. 2. Glassy-phase/ $\beta$ -phase PL relative intensity as a function of the exposure time to solvent (symbol). The continuous lines are the best fit curves with the model described in text.

tional to the number of absorbing molecules  $N_g$  and  $N_\beta$ , they can be rewritten as  $g_g = k_g N_g$  and  $g_\beta = k_\beta N_\beta$ . The FRET rate is proportional to the total number of acceptor ( $\beta$ -phase) molecules; thus,  $1/\tau_{FRET} = a_{FRET} N_\beta$ .

Moreover, the phase transition does not change the total number of molecules  $N_T$  but only the relative amount of glassy- and  $\beta$ -phase molecules. The total numbers of glassy- and  $\beta$ -phase molecules are then given by  $N_g = (1 - f_\beta) N_T$  and  $N_\beta = f_\beta N_T$ , where  $f_\beta$  is the fraction of molecules with the  $\beta$ -phase geometry.

The steady state solution for the PL intensity of the glassy phase relative to the  $\beta$ -phase one is given by

$$\frac{I_{PL_g}}{I_{PL_\beta}} = \frac{n_g}{n_\beta} \frac{\tau_{\beta rad}}{\tau_{g rad}} = \frac{A e^{-bt^n}}{1 - e^{-bt^n} + B(1 - e^{-bt^n})^2}, \quad (3)$$

where  $\tau_{i rad}$  ( $i = g$  or  $\beta$ ) is the radiative recombination time for the glassy and  $\beta$ -phases, respectively, and

$$A = \frac{\tau_{\beta rad} k_g \tau_g}{\tau_{g rad} \tau_\beta} \frac{1}{k_\beta + a_{FRET} N_T k_g \tau_g}, \quad (4)$$

$$B = \frac{N_T a_{FRET} \tau_g (k_\beta - k_g)}{k_\beta + a_{FRET} N_T k_g \tau_g}. \quad (5)$$

In the last formula, we considered an Avrami-type<sup>25,26</sup> time dependence of  $f_\beta = 1 - e^{-bt^n}$ , which is usually used to describe nucleation and growth kinetics, where  $b$  contains the rate constant which is dependent on temperature and  $n$  is the Avrami exponent which is dependent on the nucleation type and growth geometry. The experimental data have been obtained from a multi-Gaussian best fit of the spectra and are well reproduced by the best fit curve (see Fig. 2) for the best fit parameters reported in Table I. In particular, we observe that for both toluene and iso-octane, a best fit value of  $n$  of about 0.5 is obtained. In order to determine the nucleation and crystallization process in the film, we remember that the Avrami coefficient is given by  $n = n_{nucl} + n_{cr} + n_{rate}$ , where  $n_{nucl} = 0$  for athermal (simultaneous) nucleation and  $n_{nucl} = 1$  for thermal (sporadic) nucleation,  $n_{cr} = 1, 2, 3$  for the growth of fibrillar rod, disk, and spheric crystals, respectively, and  $n_{rate} = 0$  if the melt-crystal contact is enough for the crystal growth and  $n_{rate} = -0.5$  if the crystallization required the mol-

TABLE I. Best fit values of  $b$ ,  $A$ ,  $B$ , and  $n$  obtained from the fitting of the experimental data with Eq. (3).

Vapor solvent	$b$	$A$	$B$	$n$
Toluene	$0.2 \pm 0.1$	$3.4 \pm 0.3$	$-0.995 \pm 0.002$	$0.6 \pm 0.1$
Iso-octane	$2.23 \pm 0.07$	$3.6 \pm 0.1$	$-0.9958 \pm 0.0001$	$0.49 \pm 0.04$

ecule diffusion to (or from) the growth site.<sup>27</sup> An overview of the Avrami coefficients for several different nucleation and crystallization processes can be found in Ref. 27. A value of 0.5 is then consistent with athermal (simultaneous) nucleation, followed by diffusion controlled growth of 1D fibrillar crystals.

This result allows us to conclude that the solvent swelling induced  $\beta$ -phase formation is different from the thermal cycling formation process, in which evidence of diffusion-free 1D crystallization was obtained.<sup>16</sup> A further interesting difference with the  $\beta$ -phase formation due to thermal cycling is relative to the  $\beta$ -phase formation times. The observed  $\beta$ -phase contents after 10 min of toluene and iso-octane vapor exposure<sup>28</sup> are 5.9% and 4.3%, respectively, which are identical to the one obtained after 12 h vapor exposure.<sup>18</sup> This result indicates that the solvent swelling induced  $\beta$ -phase formation is basically completed in a few minutes, which is much faster than the times of several hours observed during thermal cycling.

Finally, in order to directly confirm our conclusion on the  $\beta$ -phase formation and to investigate the effects of the  $\beta$ -phase formation on the microscopic photoluminescence properties of the samples, we repeated the experiment of vapor exposure by imaging the PL variation during the phase transition with a confocal microscope. The PL maps of the toluene vapor exposed sample (Fig. 3) clearly show the presence of micrometric  $\beta$ -phase clusters and a wide uniform

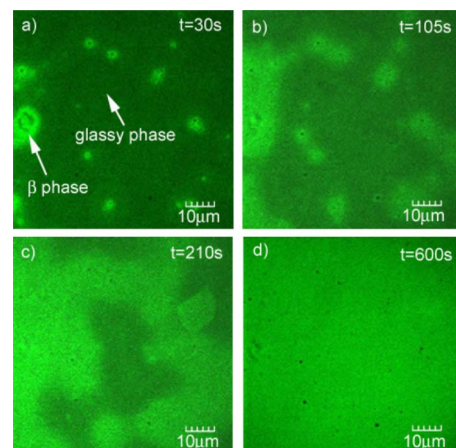


FIG. 3. (Color online) Confocal PL map of a  $72 \times 72 \mu\text{m}^2$  sample region during the exposure to toluene vapor. (a) Initially, the film shows a wide uniform glassy-phase region with micrometric  $\beta$ -phase clusters. The  $\beta$ -phase clusters act as nucleation centers for the  $\beta$ -phase formation, as shown by the size increase of the  $\beta$ -phase regions after (b) 105 s and (c) 210 s. (d) After 600 s, uniform  $\beta$ -phase emission is observed.



glassy-phase region.<sup>18</sup> The glassy- and  $\beta$ -phase regions have been identified by measuring the local PL spectra, as reported in Ref. 18. During the vapor exposure, these clusters act simultaneously as nucleation centers for the  $\beta$ -phase formation, thus leading to a size increase of the  $\beta$ -phase emitting regions of the samples that extend until the sample emission becomes uniform and dominated by the  $\beta$ -phase emission, after about 4 min. These results are consistent with the simultaneous nucleation process determined by the Avrami best fit exponent.

In conclusion, we investigated in real time the  $\beta$ -phase formation in PF8 thin film during the exposure to three solvents, namely, toluene, iso-octane, and *n*-butyl alcohol. We

demonstrate that the solvent induced swelling takes place within a few minutes, while no  $\beta$ -phase is formed by exposure to nonsolvents. We conclude that the  $\beta$ -phase is formed by athermal nucleation, followed by diffusion limited growth of 1D fibrillar crystals. This conclusion is confirmed by the PL imaging during the  $\beta$ -phase formation, showing the simultaneous  $\beta$ -phase nucleation starting from submicrometric  $\beta$ -phase clusters.

We are pleased to acknowledge P. Cazzato for valuable technical assistance, G. Ciccarella for enlightening discussions, and R. Cingolani for the use of the NNL laboratory facility.

\*Corresponding author. marco.anni@unile.it

- <sup>1</sup>J. H. Burroughes, D. D. C. Bradley, A. R. Brown, R. N. Marks, K. Mackay, R. H. Friend, P. L. Burns, and A. B. Holmes, *Nature (London)* **347**, 539 (1990).
- <sup>2</sup>N. Tessler, G. J. Denton, and R. H. Friend, *Nature (London)* **382**, 695 (1996).
- <sup>3</sup>A. Assadi, C. Svensson, M. Willander, and O. Ing nas, *Appl. Phys. Lett.* **53**, 195 (1988).
- <sup>4</sup>M. T. Bernius, M. Inbasekaran, J. O'Brien, and W. Wu, *Adv. Mater. (Weinheim, Ger.)* **12**, 1737 (2000).
- <sup>5</sup>A. W. Grice, D. D. C. Bradley, M. T. Bernius, M. Inbasekaran, W. Wu, and E. P. Woo, *Appl. Phys. Lett.* **73**, 629 (1998).
- <sup>6</sup>F. Hide, M. A. Diaz-Garcia, B. J. Schwartz, M. R. Andersson, Q. Pei, and A. J. Heeger, *Science* **273**, 1833 (1996).
- <sup>7</sup>G. Heliotis, D. D. C. Bradley, G. A. Turnbull, and I. D. W. Samuel, *Appl. Phys. Lett.* **81**, 415 (2002).
- <sup>8</sup>J. J. M. Halls, A. C. Arias, J. D. Mackenzie, W. Wu, M. Inbasekaran, E. P. Woo, and R. H. Friend, *Adv. Mater. (Weinheim, Ger.)* **12**, 498 (2000).
- <sup>9</sup>H. Sirringhaus, R. J. Wilson, R. H. Friend, M. Inbasekaran, W. Wu, E. P. Woo, M. Grell, and D. D. C. Bradley, *Appl. Phys. Lett.* **77**, 406 (2000).
- <sup>10</sup>W. Chunwaschirasiri, B. Tanto, D. L. Huber, and M. J. Winokur, *Phys. Rev. Lett.* **94**, 107402 (2005).
- <sup>11</sup>A. Hayer, A. L. T. Khan, R. H. Friend, and A. K hler, *Phys. Rev. B* **71**, 241302(R) (2005).
- <sup>12</sup>O. J. Korovyanko and Z. V. Vardeny, *Chem. Phys. Lett.* **356**, 361 (2002).
- <sup>13</sup>C. Rothe, F. Galbrecht, U. Scherf, and A. Monkman, *Adv. Mater. (Weinheim, Ger.)* **18**, 2137 (2006).
- <sup>14</sup>M. Ariu, M. Sims, M. D. Rahn, J. Hill, A. M. Fox, D. G. Lidzey, M. Oda, J. Cabanillas-Gonzalez, and D. D. C. Bradley, *Phys. Rev. B* **67**, 195333 (2003), and references therein.
- <sup>15</sup>A. L. T. Khan, P. Sreearunothai, L. M. Herz, M. J. Banach, and A. K hler, *Phys. Rev. B* **69**, 085201 (2004).
- <sup>16</sup>M. J. Winokur, J. Slinker, and D. L. Huber, *Phys. Rev. B* **67**, 184106 (2003).
- <sup>17</sup>M. Anni, M. E. Caruso, S. Lattante, and R. Cingolani, *J. Chem. Phys.* **124**, 134707 (2006).
- <sup>18</sup>M. E. Caruso, S. Lattante, R. Cingolani, and M. Anni, *Appl. Phys. Lett.* **88**, 181906 (2006).
- <sup>19</sup>J. Hill, S. Y. Heriot, O. Worsfold, T. H. Richardson, A. M. Fox, and D. D. C. Bradley, *Phys. Rev. B* **69**, 041303(R) (2004).
- <sup>20</sup>T. Virgili, D. Marinotto, C. Manzoni, G. Cerullo, and G. Lanzani, *Phys. Rev. Lett.* **94**, 117402 (2005).
- <sup>21</sup>A. J. Cadby, P. A. Lane, H. Mellor, S. J. Martin, M. Grell, C. Giebeler, D. D. C. Bradley, M. Wohlgenannt, C. An, and Z. V. Vardeny, *Phys. Rev. B* **62**, 15604 (2000).
- <sup>22</sup>A further contribution to the differences in the  $\beta$ -phase formation times can be related to a different permeability of toluene and iso-octane vapors in the PF8 glassy films. Such differences have been reported for glassy polyimide membranes (Ref. 23) but no data are available in literature for polyfluorene membranes.
- <sup>23</sup>J. Hao, K. Tanaka, H. Kita, and K. Okamoto, *J. Membr. Sci.* **132**, 97 (1997).
- <sup>24</sup>E. J. M. List, R. G ntner, P. Scanducci de Freitas, and U. Scherf, *Adv. Mater. (Weinheim, Ger.)* **14**, 374 (2002).
- <sup>25</sup>M. Avrami, *J. Chem. Phys.* **7**, 1103 (1939).
- <sup>26</sup>M. Avrami, *J. Chem. Phys.* **8**, 212 (1940).
- <sup>27</sup>P. C. Hiemenz, *Polymer Chemistry: The Basic Concepts* (Dekker, New York, 1984).
- <sup>28</sup>Estimated from the absorption band areas assuming the same oscillator strength for the glassy- and  $\beta$ -phase absorption.